MULTISCIA JOURNALS PUBLISHERS

FRONTIERS IN MATERIAL SCIENCE AND NANOTECHNOLOGY

ISSN: (3065- 4114)

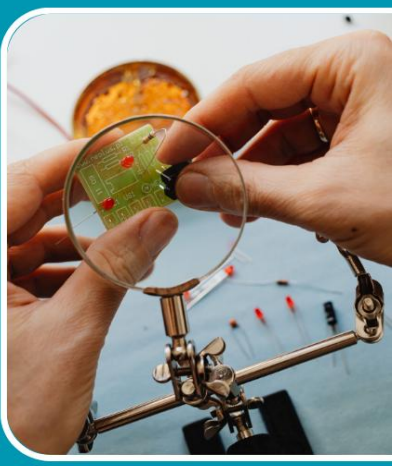

editor.fmsnt@gmail.com

https://multisciajournals.com/journals/index.php/fmsnt

Organic Pollutant Degradation in Water via Plasmon Mediated Photocatalysis Using Solar Active Ag/ZnO Nanostructures

K, Kshirsagar jii
Department of Material Science and Nanotechnology

Article Info

Received: 29-09-2025 *Revised:02-11-2025* *Accepted:11-11-2025* *Published:24-11-2025*

Abstract

The topic of this study is the efficient treatment using an in-situ produced Ag/ZnO nano catalyst. Zinc oxide nanoparticles with a plate shape were produced during catalyst production by using starch as an eco-friendly surfactant. X-Ray Diffraction analysis verifies the presence of hexagonal ZnO and fcc silver in the as-synthesized catalyst. XRD analysis also showed that the crystal structures of ZnO and Ag/ZnO are accurate, with d-spacings of 0.26 nm and 0.234 nm, respectively. Because starch was present, the morphology shown by FESEM, EDX, and TEM was spherical but flat plate type. UV-Vis spectrophotometry showed a reduction in band gap energies with increased silver loading, and XPS verified the composition's oxygen richness. Sunlight was used to study the plasmonic catalysts' photocatalytic activity. Using absorption spectroscopy, we were able to see the full degradation of organic dyes such as p-nitrophenol (PNP), Methylene Blue (MB), Rhodamine B (RhB), Methyl Orange (MO), and Bromophenol Blue (BPB) in aqueous solutions. The catalyst's characteristics were maintained even after the third recycling. An easy way to cure effuently in the sun might be using this simple catalyst.

Keywords: Plasmonic Photocatalysis; Semiconductor; Advanced Oxidation Process; Dye Degradation

Introduction

Since Fukushima and Honda's 1971 achievement of water splitting with TiO2 under light irradiation [1], researchers have extensively studied the photocatalytic activity of semiconductor materials. Since they are readily available, non-toxic, thermally and chemically stable, and have several uses (e.g., photo-degradation of organic pollutants [5,6], artificial photosynthesis [7], and water splitting [8]), semiconductors TiO2 and ZnO have garnered a lot of attention as photocatalytic reaction materials. Although ZnO and TiO2 have a comparable band gap energy (~3.2 eV), ZnO is better in degrading water pollutants [9]. Photocatalytic degradation processes may be carried out more efficiently by ZnO due to its lower electric potentials in the valence and conduction bands (-0.45 to 2.75 eV) compared to TiO2 (-0.1 to 3.1 eV) [10,11]. As an additional benefit, ZnO has more quantum efficiency than TiO2 when used as a photocatalyst to degrade contaminants in water [12]. Since photocatalytic degradation converts organic contaminants to carbon dioxide and water without producing any hazardous by-products, it is an eco-friendly process [13,14]. It is common practice to conduct laboratory photocatalytic reactions under xenon lamp illumination rather than in natural sunlight to ensure accurate catalyst performance testing. Direct sunshine, of which 50% is UV radiation, is ideal for conducting degradation studies, as it improves the process's attractiveness. The band-gap properties of ZnO restrict its UV activity to the 3–4% solar spectrum. The optical properties of ZnO need to be adjusted within the visible range, namely between 400 nm and 700 nm, in order for it to function as an efficient catalyst in the visible area, which receives around 44% of the sun's energy [15]. Creating structural flaws [16], synthesising particles of varied morphologies, doping, etc., are only a few of the many strategies used to change the band-gap of ZnO. Nanorods [18], nanoflowers [19], nanowires [20], and nanosheets [21] are just a few examples of the different shaped and sized nanoparticles that have been synthesized to enhance their crystalline quality and make them more useful as visible light photocatalysts.One eco-friendly and efficient surfactant alternative is bio-polymers like starch, which are used to regulate the size and form of particles. Starch is a green precursor and an economically feasible choice for producing ZnO; its polymeric nature reportedly serves as a template for the development of highly crystalline nanoparticles [22-25].

One of the most effective semiconductor photocatalysts, TiO2 has been employed widely according to literature sources. The main obstacle to achieving high photocatalytic effectiveness against pollutants is the rapid recombination of charge carriers when exposed to light. The quantum efficiency of photocatalysis is diminished due to the quicker kinetics of electron and hole pair recombination. It is crucial to reduce the recombination rate to increase the photocatalysis efficiency. Changing the surface charge, functionality, reactivity, and stability of the photocatalyst may alleviate this photocorrosion issue. Several papers have detailed the restriction of photocorrosion by surface modification; here we will examine a few key examples. Zhu et al. [25] successfully reduced photocorrosion by combining ZnO with graphite-like carbon. The improvement of catalytic activity and reduction of photocorrosion caused by surface modification is detailed in another study on photoelectrochemical water splitting using carbon

and nitrogen co-treated ZnO nanorod arrays. Photocatalysis demonstrated promising outcomes when ZnO was coupled with carbon materials and decreased graphene oxide, leading to improved photocatalytic activity and reduced photocorrosion [26]. You may also think about doping ZnO [26] with metals [27], non-metals [28], other chemicals [29], or semiconductor materials [15] to boost its visible range photocatalytic activity. The most desirable of these is the use of noble metal doping, such as Ag or Au, because of light-induced photoluminescence (LSPR), a feature that is exclusive to noble metal conduction band electrons. Doping with noble metals, such as silver, reduces electron-hole recombination [30] by creating a Schottky circuit; catalysts doped with noble metals are often called plasmonic photocatalysts [31,32]. Multiple studies have examined Ag-doped ZnO, (e.g. By tracking the degradation response of Rhodamin 6G (R6G), Georgekutty et al. [33] documented the visible light performance of Ag doped ZnO particles. While Mondal [34] et al. monitored a spectrum of dyes to study the direct sunlight performance of ZnO photocatalysts doped with Au, the degradation efficiency was not appealing. Using starch as a surfactant, Zhang et al. [22] created microporous ZnO with high crystallinity that exhibited remarkable UV catalytic activity. Research showed that semiconductors with a high oxygen concentration were more effective as visible light photocatalysts. Even though Ag/ZnO may be synthesized in a single pot, a great alternative would be to precipitate the silver nanoparticles onto the surface, as this would allow for more control over the particle concentration. Here, the authors expand their work in photocatalysis, building on their prior demonstrations of the manufacture and uses of ZnO, TiO2, and silver nano-particles [22]. Sintering starch at a lower temperature to preserve oxygen-rich surfaces is fundamental to the current study's creation of a highly solar-active silver-doped ZnO photocatalyst. Methylene Blue was selected as the principal dye for the purpose of studying the photocatalytic performance. Additional organic dye degradation processes were seen for p-nitrophenol, bromophenol blue, methyl orange, and Rhodamine B. Solar degradation of p-nitrophenol using Ag doped ZnO is described in this study for the first time, as far as we are aware.

Experimental

Materials

All reagents used were of analytical grade and were purchased from commercial sources. The water used for the experiment is ultrapure water from Millipore Direct Q 3UV purifier system.

Instrumentation

The Bruker A8 advanced with monochromatized CuKα radiation, an accelerating voltage of 40 kV, and an applied current of 20 mA were used to conduct the powder X-Ray diffraction. To determine the nanocrystal composition, a supra 40, Carl Zeiss Pvt. Ltd. Instrument, and an Oxford Link, ISIS 300 were used for field emission scanning electron microscopy (FESEM) and energy dispersive atomic scattering (EDAX), respectively. Researchers used an Agilent Cary Eclipse fluorescence spectrophotometer to measure photoluminescence. The photos were captured using a TECHNAI G2 apparatus, which is a transmission electron microscope (TEM). The ESCA-3000, manufactured by VG Microtech UK, was used for X-Ray Photoelectron Spectroscopy (XPS), which used Mg Kα and Al Kα sources. We used a Specord 210 plus (Analytik Jena) for all of our ultraviolet-visible spectroscopic investigations. A Lutron LX-101A light meter was used to measure the intensity of the sunshine. Direct sunshine with an average intensity of around 86,500 LUX, as measured by a LUX meter, was used to conduct the photocatalytic activities.

Synthesis of ZnO nanoparticles

A 0.5% starch solution was mixed with 30.00 g of zinc nitrate [11] and stirred continuously for one hour. Following the zinc nitrate's full dissolution, the reaction mixture was heated to 60 °C and 600 ml of a NaOH solution in water (0.2 M) was added. For a further four hours, the mixture was mixed continuously at the same temperature. Overnight, the whole mixture was allowed to cool and age. The solution underwent centrifugation to extract a white precipitate, which was then washed twice with distilled water and ethanol. The resulting white powder was then dried in an oven set at 80 °C for three to five hours. **Nanocatalyst for Ag/ZnO Synthesis**

After 30 minutes of sonication, 100 milliliters of ethanol was used to disperse 1 gram of ZnO nanoparticles. The aforementioned solution was used to prepare Ag/ZnO 1 by dissolving 40 mg of AgNO3. A brownish-yellow precipitate was obtained by stirring the solution at 45 °C for three hours. Centrifugation was used to collect the precipitate, which was then washed with ethanol and DI water. In a similar vein, 160 mg of AgNO3 was added to a solution or suspension containing the same quantity of ZnO to make Ag/ZnO 2. **Exploring photocatalysis**

Seeing how quickly methylene blue dye degraded in sunshine allowed us to gauge the Ag/ZnO composition's photocatalytic activity. A solution of methylene blue in water with a concentration of 0.02 mM was made using distilled water. A final reaction solution (1g/L) was prepared for photocatalytic assessment by dispersing 30 mg of bare ZnO or

Ag/ZnO catalysts into 30 mL of methylene blue solution. For 20 minutes, the solutions were agitated vigorously and held in the dark until the MB and catalyst surfaces reached an adsorption equilibrium. The mixture was stirred occasionally when left in direct sunshine. Following the reaction, the sample's UV/Vis spectra were recorded by centrifuging 2 mL of solution every 20 minutes. Various concentrations of catalysts were used to repeat the operation. The following substances were also tested in the same manner: p-nitrophenol, Rhodamine B (RhB), Methyl Orange (MO), and Bromophenol Blue (BPB).

Results and Discussion

White crystalline nanoparticles of ZnO is formed as the result of the reaction.(A in Figure 1). During reaction Zn ions of Zinc Nitrate interact with OH radicals of starch networks, which is an important component of the system [24]. The zinc oxide formed get converted to ZnO nanoparticles by heat treatment at 100-200 °C. The nitrate group get decomposed as NO_2 and Oxygen.

The typical reaction can be expressed as:

$$Zn(NO_3)_2.\ 6\ H_2O + 2NaOH \rightarrow 2NaNO_3\ (aq.) + Zn(OH)_2 + 6H_2O \quad .....(1)$$

$$Zn\ (OH)_2 \rightarrow ZnO + H_2O \quad .....(2)$$

Figure 1: As-synthesized ZnO (A), Ag/ZnO **1** (B) and Ag/ZnO **2** (C) nanoparticles

Suspension of ZnO particles capped with starch was made in ethanol and $AgNO_3$ was added to it for loading of silver particles via reduction of silver ions. The process involves reduction of silver salt by the ethanol solution whereby Ag particles are formed on the surface of ZnO. Ethanol is known to be a mild reducing agent and formations of silver nano-particles have been reported by ethanol reduction process by others also [35]. The color changes from white to mild yellow and/or yellow brown for the final silver doped zinc oxide powders (B, C in Figure 1). The typical chemical reaction mechanism could be explained as below;

$$AgNO_3 + C_2H_5OH + ZnO \rightarrow Ag^+ + NO_3^- + ZnO + C_2H_5O^- + H^+ \quad .....(3)$$

$$Ag^+ + e^- + ZnO \rightarrow Ag^0 \quad /ZnO \quad .....(4)$$

The so-generated powders were analyzed by several modern tools e.g. XRD, SEM, TEM, XPS, UV-Vis and PL spectroscopy.

XRD Measurements

A powder X-ray diffraction (PXRD) analysis was performed on the as-prepared samples to ascertain their crystallinity, phase, and purity. As illustrated in Figure 2a, the XRD patterns of the ZnO and ZnO/Ag particles were found. The hexagonal ZnO structure has ten significant peaks at certain 2θ values: 31.82, 34.47, 36.29, 47.56, 56.53, 62.89, 66.35, 67.96, 69.15, 72.56, and 77.46º. These peaks correspond to the (100), (002), (101), (102), (110), (103), (200), (112), (201), and (202) crystal planes, respectively [22]. There are no structural changes owing to silver doping, since the same peaks present in the XRD pattern of Ag/ZnO. However, the pattern also exhibits peaks for fcc Ag. An good proof of the synthesis of silver at ZnO was provided by a peak at 2θ 38.45º, which is caused by the presence of the (111) crystal plane of silver particles on the surface of the material [18]. The XRD pattern shows a very faint hump, and the peak at 2θ 44.27º for (200) is also evident, while the peak at 2θ 64.60º for (220) is less distinct. The crystal planes of fcc metallic Ag are not very obvious. Figure 2b shows that in the presence of silver, there is a little red shift in the 2 theta values of the ZnO peaks, which may be the result of intera- the creation of a Schottky connection between the silver and the ZnO matrix [36]. Using the Debye-Scherrer equation [22], we were able to determine that the nanoparticles were 21.6 nm in size. Thanks to the incorporation of Ag particles into the matrix, the crystalline size of Ag/ZnO increased slightly but noticeably [37]. With an estimated silver particle size of 18.9 nm, either on the surface or in the ZnO matrix, the metal is likely to be adsorbed on the material. At a 2θ value of 34.47º, the lattice gap between the 002 plane and the other plane in ZnO is 0.26 nm. For 111 silver planes at a 2θ value of 38.45º, the same is true for the silver contained in the Ag/ZnO catalyst: 0.234 nm. The lattice spacings of the two materials are in good agreement with the stated values, which verifies the nanoparticles' high quality and their real crystal planes and structure [17]. The availability of oxygen vacancies inside the ZnO crystal structure is a key factor in determining its catalytic activity. Reports in the literature verified the presence of oxygen vacancies in this particular instance [37].

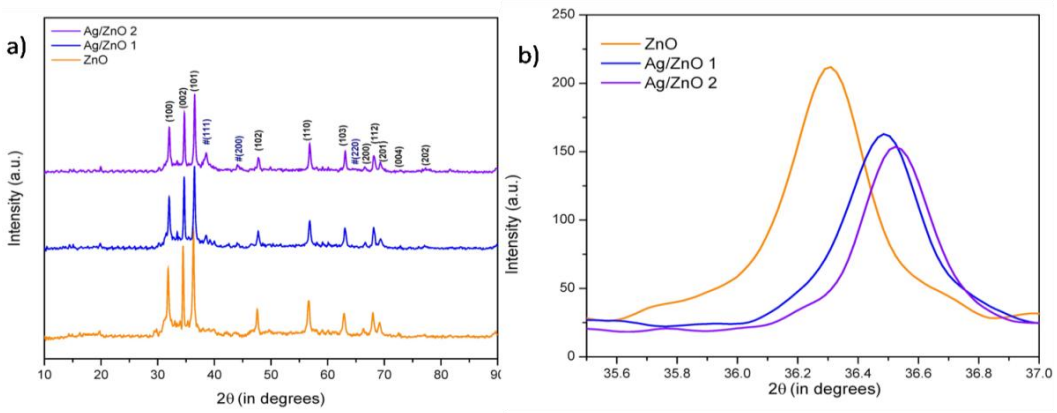

Figure 2: XRD patterns of various samples (a) ZnO and Ag/ZnO (b) 101 plane of same.

SEM/EDAX Analysis

To study the morphology of ZnO particles and distribution of Ag particles on the surface of the matrix, SEM analysis was carried out (Figure 3). In the SEM image, the morphology of the matrix (ZnO) is observed to be plate like however flaky in nature but closer to tubular shaped. Such mixed elongated morphology has been described to be useful for energy capturing process [38]. The Ag doped ZnO showed spherical particles on the surface of the plate like flakes which no longer retains tubular appearance but are elongated to retain mixed morphology of the powder. The surface of the ZnO nanoparticles can be seen with uniformly dispersed Ag nanoparticles all over them. The Ag particles are more visible in the sample with larger concentration than the one with lower concentration.

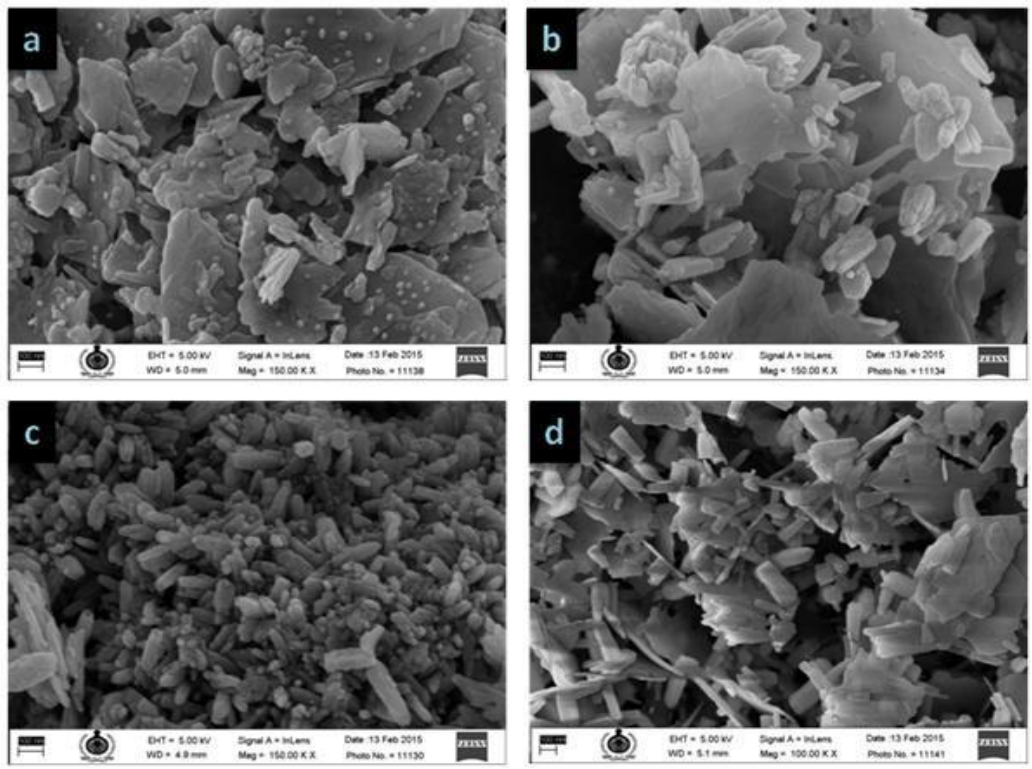

Figure 3: SEM of as-prepared a) Ag/ZnO 2; b, c) Ag/ZnO 1; d) ZnO (scale bar 100 nm)

Two clear silver percentages could be established with the help of EDAX analysis (Figure 4) e.g. the experiment conducted with lower concentration (40 mg) of silver salt resulted in close to 1% (0.89%) Ag loading on ZnO. However sample prepared with large concentration (160 mg) of $AgNO_3$ showed about 4% (3.89%) of Ag loading (Table 1). It is clear from EDAX analysis that only approximately 1 and 4% loading was completed. This indicates that, ethanolic reduction is indeed slow and during the reaction time, only about 40% much reduction was possible. It is found that Zn:O ratio is non-stoichiometric which can be because of the presence of starch thereby giving oxygen rich surfaces. It has been already described that oxygen rich TiO_2 is more effective as a photocatalyst [2]. In the present case too, this may stand valid for effective photo degradation of the organic during the photocatalytic process.

EDAX	ZnO		Ag/ZnO 1		Ag/ZnO 2	
Element	Weight %	Atomic %	Weight %	Atomic %	Weight %	Atomic %
O K	42.13	74.84	34.41	68.31	34.81	69.09
Zn K	57.87	25.16	64.70	31.43	61.27	29.76
Ag L	--	--	0.89	0.26	3.92	1.15

Table 1: Elemental composition from EDAX analysis

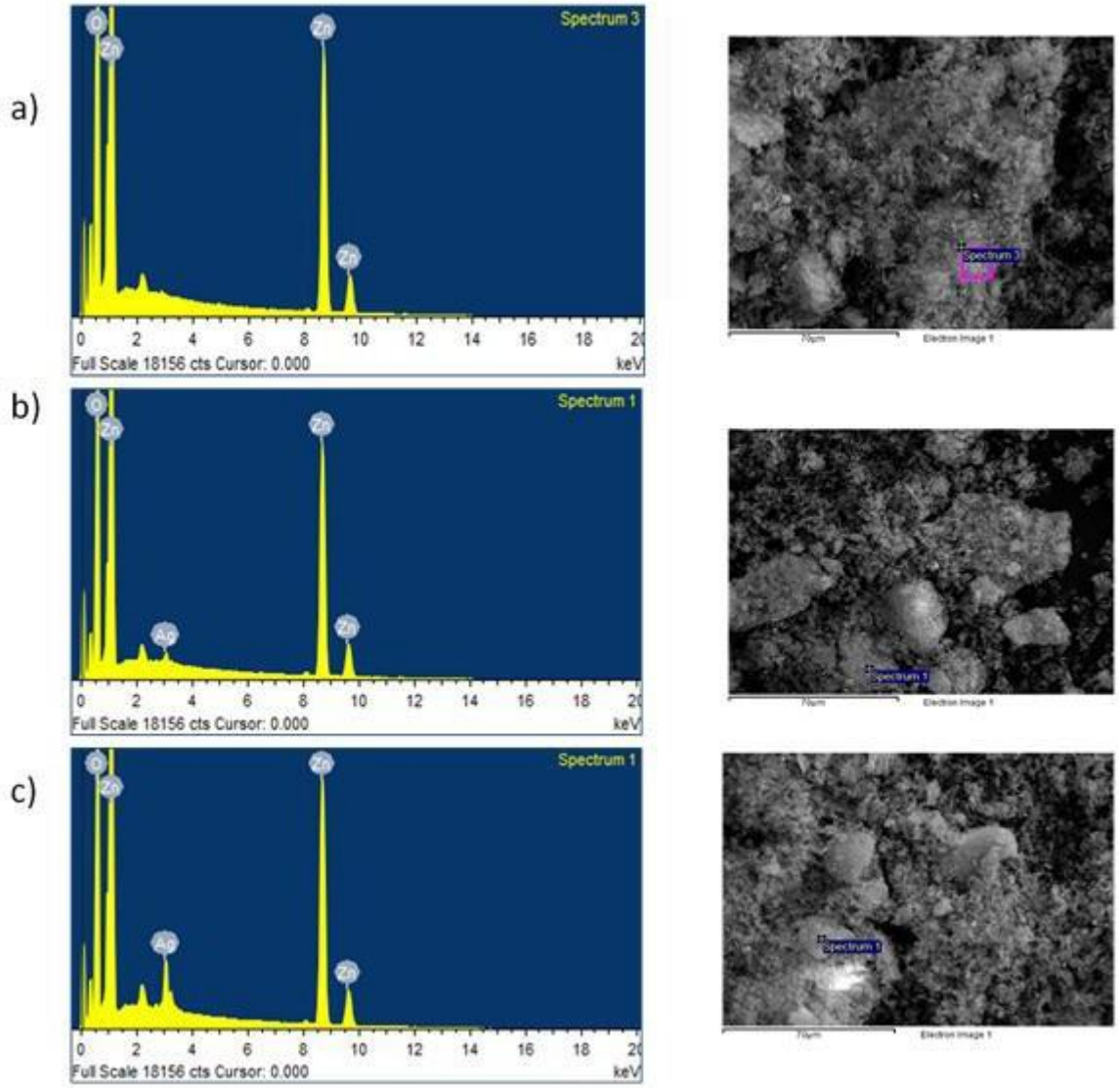

Figure 4: EDAX spectrum of a)ZnO b)Ag/ZnO 1 c)Ag/ZnO 2

SEM/EDAX Analysis

In the TEM images, the sample showed large plate and flaky appearance. The matrix plates (starch) are about 150-200 nm in length and about 20 nm in width. However uniformly distributed much smaller particle of ZnO can be considered due to presence of starch as overall matrix (Figure 5). The dark spots observed are due to homogeneously distributed silver nanoparticles on the surface of ZnO with the particle size of 15-20 nm. It is seen that ZnO is mostly appear as rod shape which match well with morphological observations made from SEM. Due to the lack of high quality HRTEM, lattice fringes for silver and zinc oxide could not be measured to demonstrate diffusion of silver to the ZnO boundary.

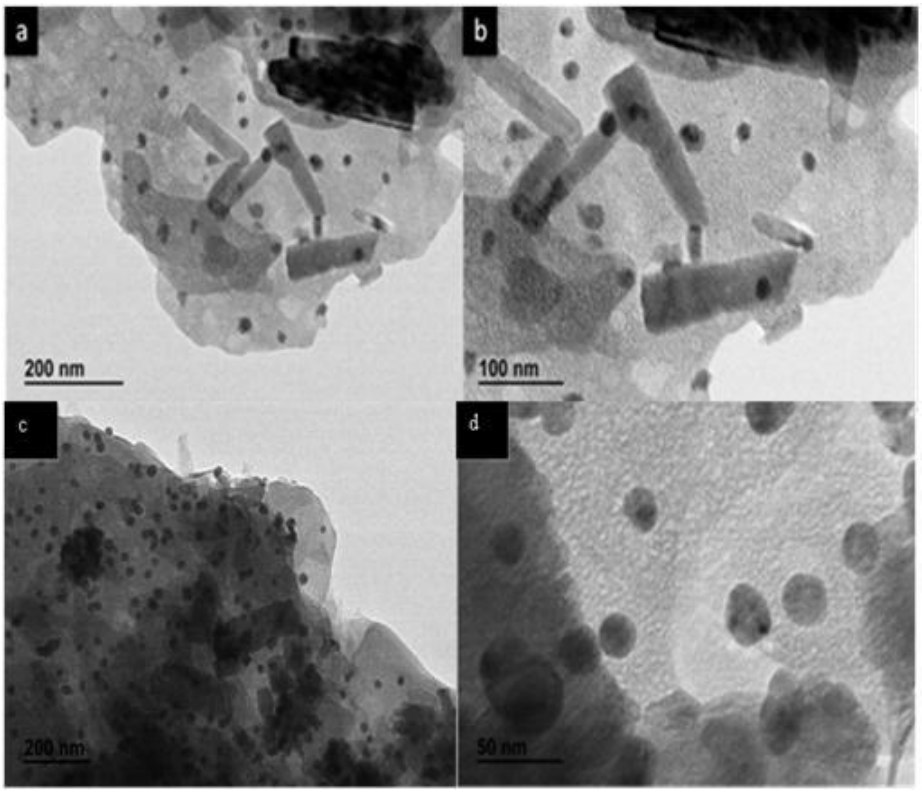

Figure 5: TEM images of as-prepared Ag/ZnO (a,b Ag/ZnO 1) (c, d Ag/ZnO 2)

XPS Analysis

We used XPS research to learn about the Ag/ZnO composite's surface components and chemical states. One possible conclusion is that, unlike undoped ZnO, which only contains Zn and O, Ag/ZnO only contains Ag, Zn, and O. The curves' calibration value is the carbon peak (C 1s) at 284.8. Zn 2p3/2 and Zn 2p1/2 are represented by the peaks at 1021.4eV and 1044.48eV, respectively, as seen in Figure 6. When Zn2+ ions are formed, it causes a splitting of the orbitals [21]. When silver is doped, the peak shows a little shift to a higher band energy. Two symmetrical signals, one representing lattice oxygen and the other surface hydroxyl oxygen, may accommodate the peak owing to oxygen O (1s) [16]. When oxygen is doped with Ag, it likewise exhibits a positive shift. There is a little departure from the bulk Ag value of 368.2 eV and 374.2 eV, respectively, and the distinctive peaks at 367.6 eV and 373.6 eV, which correspond to Ag 3d5/2 and 3d3/2, respectively, are given by silver. The reduction of Ag metal to form metallic silver is shown by the 6eV difference between two orbitals of Ag [18]. As the electron density of Ag decreases, the binding energy shifts to a lower value relative to pure silver. The reduction in the size of Ag's work function causes electron transport from the Ag layer to the ZnO surface's conduction band. This results in the formation of an energy level that signifies a strong contact between the Ag and ZnO particles. The interaction between zinc oxide and silver may explain why zinc and oxygen undergo positive shifts whereas silver undergoes negative shifts. The change to lower energy levels for silver must be due to the reduced binding energy of monovalent Ag compared to zerovalent Ag [39].

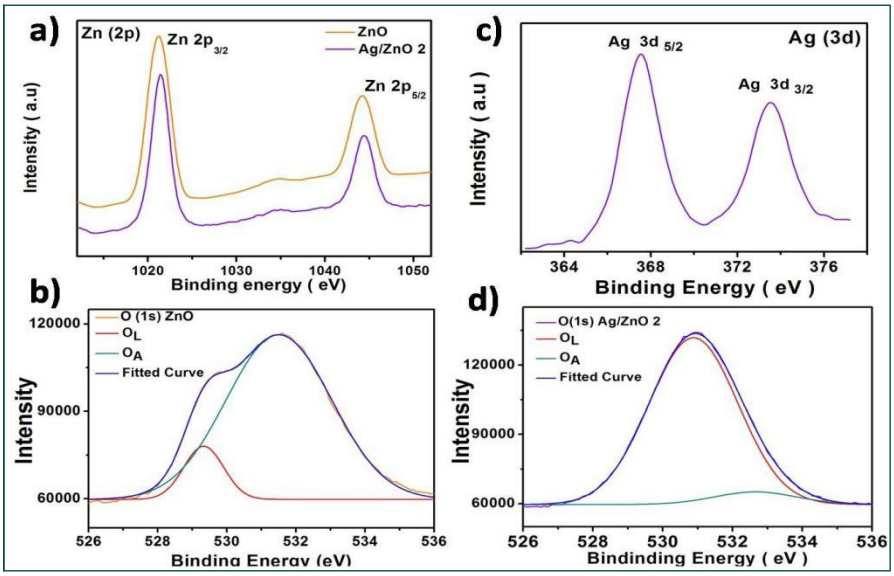

Figure 6: XPS patterns of ZnO and Ag/ZnO **2** a)Ag 3d spectrum b)Zn (2p) Oxygen spectrum of c) ZnO and d)Ag/ZnO **2**

UV/Vis Spectroscopy

UV-Vis spectroscopy was performed to study the optical properties of ZnO nanoparticles after Ag doping. Pure ZnO particles gave rise to a peak at 373 nm which is similar to many reported values and is blue shifted by about 10-15 nm with respect to bulk value. Upon addition of the Ag nanoparticle to the ZnO, a minor red shift in ZnO peak is noticed. In the case of sample with largest concentration of Ag, an additional hump for silver nano-particles is observed at 429 nm due to localized surface Plasmon resonance (LSPR) and can indicate the morphology of silver particles close to spherical (Figure 7a). LSPR of Ag in ethanol is observed around 409 nm [40] and it finally settled at 429 when loaded in ZnO. This observation indicates a slight aggregation as well as increase in particle size. The Plasmon absorption peak is inversely proportional to the root of electron density of the metal [19]. Thus it is likely that LSPR will shift due to the transfer of electrons from silver to zinc oxide through ZnO-O..Ag structural arrangement in situ. Since silver has got a smaller work function than ZnO, the transfer of electron will take place from Ag to conducting band of ZnO to achieve Fermi level equilibrium [37].

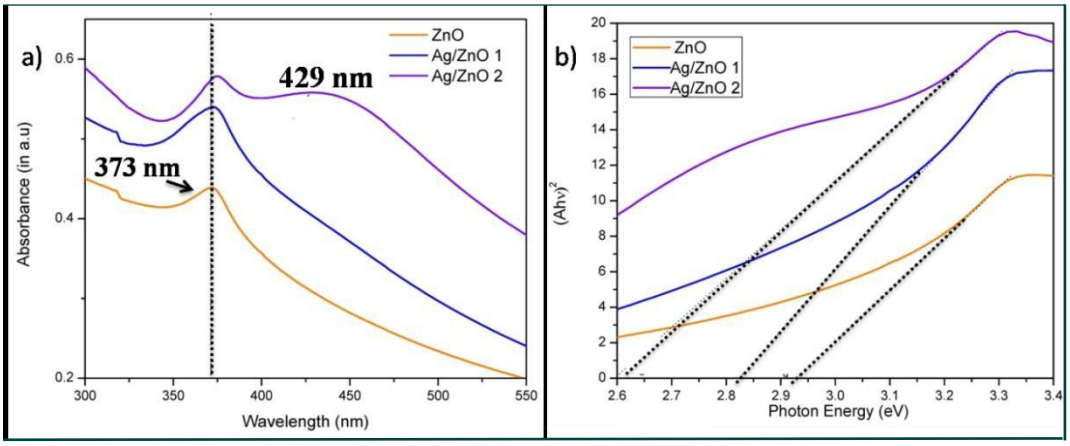

Figure 7: (a) UV/Vis Spectrum b) Tauc diagram of ZnO and Ag/ZnO samples

The hν values were plotted against $(\alpha h\nu)^2$ and extended to calculate the bandgap of the nanoparticles by Tauc method [36]. The band gap (Eg) of the ZnO was calculated to be 2.9 eV, however for the 1% and 4% Ag doped ZnO, a reduction was observed possibly due to oxygen richness on ZnO surfaces. Addition of Ag reduced the bandgap by about 0.1-0.3 eV to be observed at 2.8 eV and 2.6 eV. The reduced eV value enabled the possibility of high photoactivity of the nanoparticles in the visible region (Figure 7b).

Pholotolumiscence Spectra

To know more about the optical properties, Pholotolumiscence data of the samples is analyzed (Figure 8). PL spectrum can provide insights on quality of crystals, structural defects (surface oxygen vacancies, Zn interstitials) and particle surfaces [39]. The room temperature PL spectrum of the samples after exciting the absorption band at 325 nm is recorded. The strong emission peak at 389 nm is the main emission along with minor emissions at 493 and 530 nm which can be due to bound excitons and oxygen deficiency respectively [33]. PL intensity decreased as the concentration of Ag increased. Lower photoluminescence intensity is an indicator of higher life time of electron hole pair. It shows that the adding Ag into the ZnO matrix inhibits the recombination rate [41].

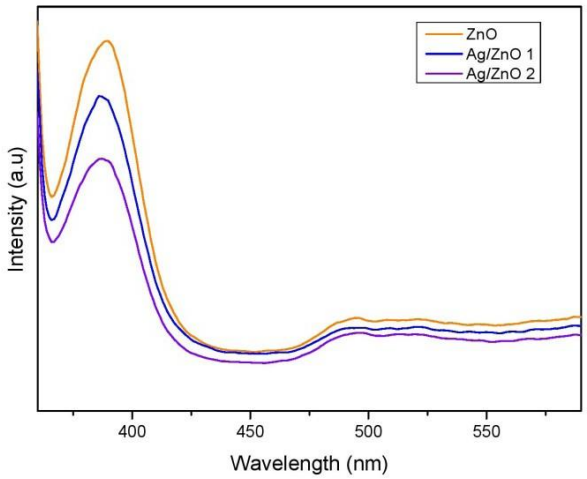

Figure 8: PL Spectra of ZnO and Ag/ZnO samples

Photocatalytic studies

The degradation of pollutants was done in direct sunlight at sunlight intensity of around 80000 lux (~590 W/m^2). Methylene Blue is a cationic Azo dye which has been widely studied as a model dye for monitoring photocatalytic reactions. Two major absorbance peaks of methylene blue in water were located at 292 nm and 664 nm, due to benzene ring and heteropolyaromatic linkage respectively. The peaks at 604 nm and 575nm are due to the formation of dimer and trimer particles of MB in aqueous condition [43]. Chemical structure of MB is given below (Figure 9a);

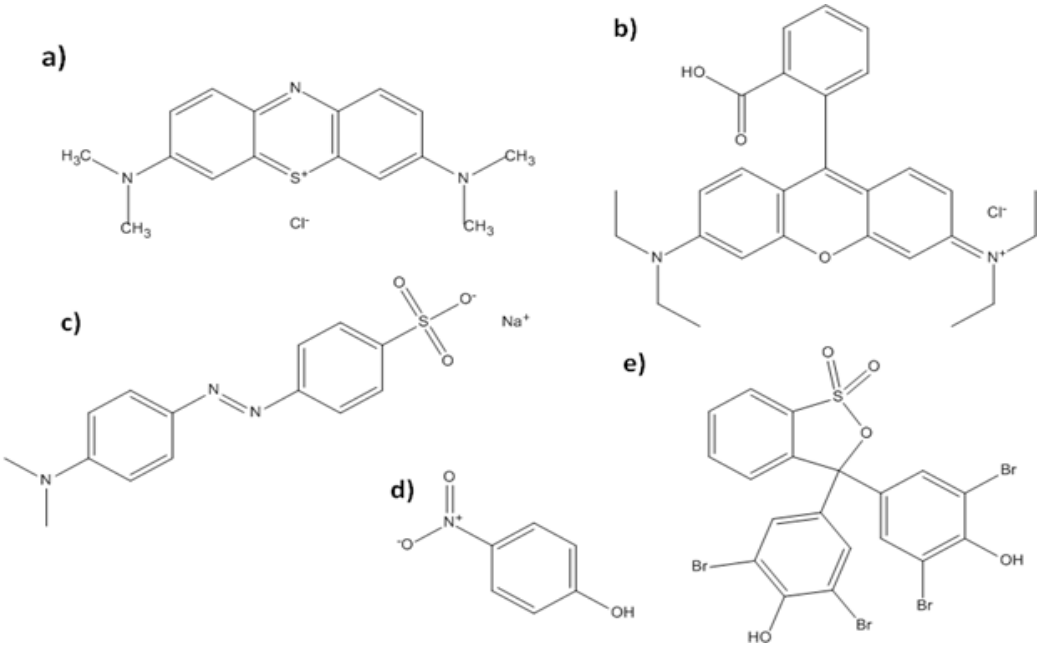

Figure 9: Chemical structure of dyes: a)Methylene Blue (MB) b)Rhodamine B (RhB), c)Methyl Orange (MO), d) p-nitrophenol (PNP) and e)Bromophenol Blue (BPB)

The photocatalytic degradation of Methylene Blue was evaluated with synthesized ZnO NPs and Ag/ZnO NPs under direct sunlight irradiation. The changes in the absorption intensity of MB (664 nm) was monitored by UV-vis spectroscopy. The photocatalytic activity of the catalyst are in the following order ZnO < Ag/ZnO 1 (1 wt %) < Ag/ZnO 2 (4 wt %). 1% Ag/ZnO improved the rate by 15%, while 4% Ag/ZnO improved it by 40%. The decolorization of MB ([catalyst] = 1.0 g L^{-1}, [MB] =0.02 mM) was achieved in 120 min in the presence of 4% Ag/ZnO under direct sunlight irradiation (Figure 10). This therefore confirms formulation of a solar light active ZnO and extremely solar light active Ag/ZnO photocatalysit. The complete degradation of Methylene Blue has been achieved with all the samples. There are no visible signs of formation of intermediates in UV degradation curves. Rate of degradation of 664nm peak is higher in the reaction thus indicating faster degradation of monomers. The MB degradation can be summarized based on the earlier reported literature as below;

$$C_{16}H_{18}N_3S + 24\,O_2 \rightarrow 16CO_2 + 3NO_3^- + SO_4^{2-} + 6H+ + 6H_2O \text{ [44]} \qquad \text{.....(5)}$$

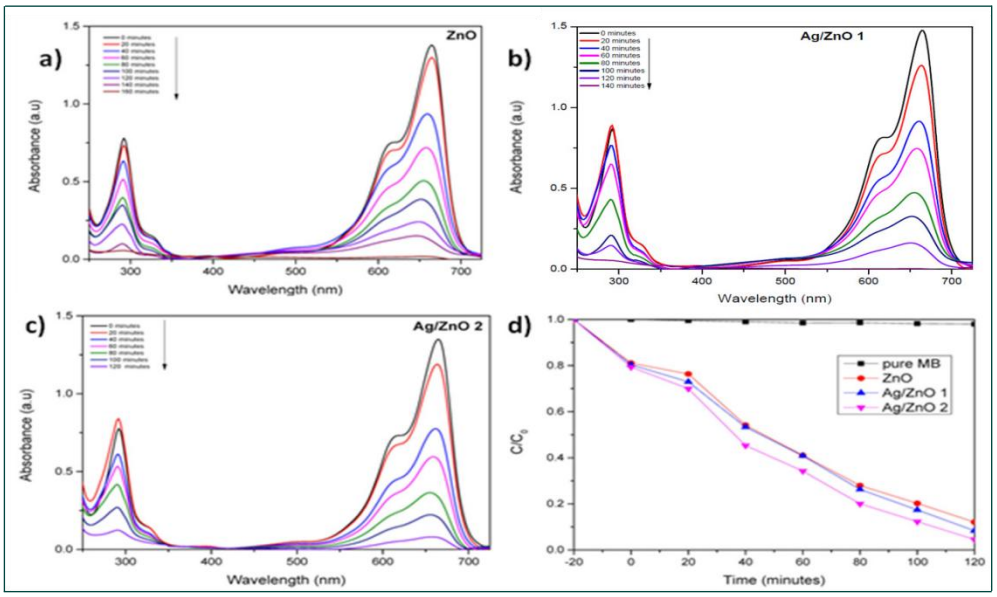

Figure 10: Degradation of MB with a) ZnO, b) 1% Ag/ZnO, c) 4% Ag/ZnO with 1.0g/Lcatalyst concentration d) C/C0 Vs time curves

The amount of catalyst required is another factor which influences the photocatalytic degradation of MB. The degradation rate was faster in reactions when the concentrations of catalyst (AgZnO) 0.5 g L^{-1} than 0.25 g L^{-1} (4%Ag). In fact the solution with the higher amount of the catalyst (1.0 g L^{-1}) should have offered more active surface area for the photocatalytic degradation of MB but surprisingly a decrease in the degradation rate was monitored which is presumably may be due to light scattering by excess amount of catalyst present [41] in the photocatalytic reaction system (Figure 11).

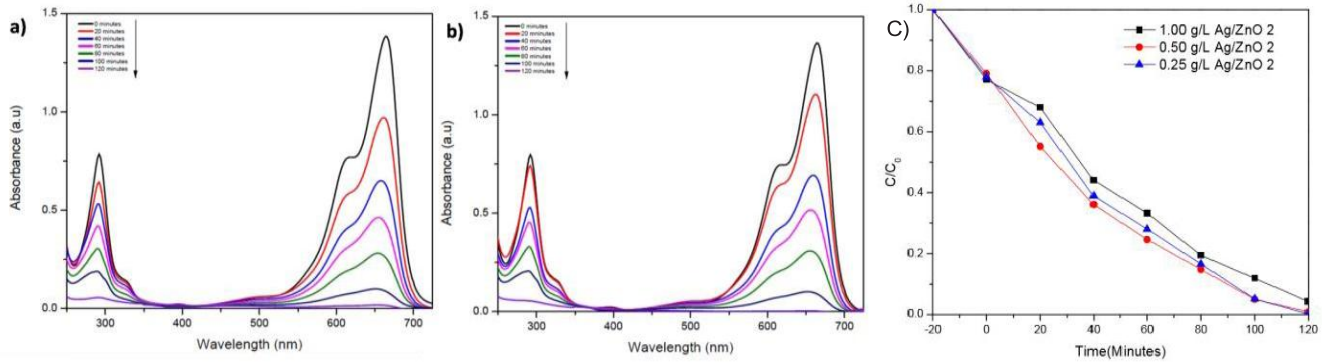

Figure 11: Degradation of MB with various concentrations of Ag/ZnO 2 a) 0.5g/l b)0.25g/l and c) C/C0 Vs time curves for degradation of MB with various concentration.

In order to study the reusability of the catalyst the reaction was repeated for four cycles. The catalyst remained highly solar active and retained around 95% of its activity. This confirms that the catalyst can be effectively used in photocatalytic reactors and can be used for commercial purposes, as the leaching of Ag in the surface is negligible (Figure 12).

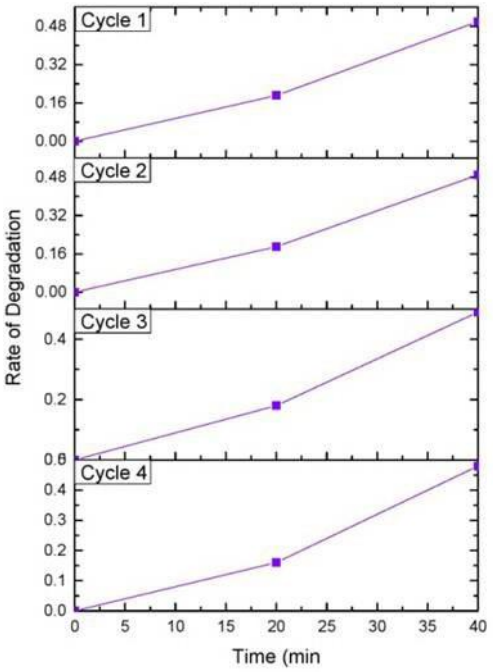

Figure 12: Recycle study of Ag/ZnO 2

Similarly, photcatalytic activities of Ag/ZnO was tested against another industrially important dye called Rhodamine B (Figure 9b). Degradation reaction of Rhodamine B was quite quick in the case of Ag/ZnO, the reaction was completed in a short time of about 80 minutes; while ZnO took twice the time to complete the degradation process. It can be concluded that the despite synthesized ZnO by the current method using starch as a surfacing agent itself is quite efficient in degradation of cationic dyes, the rate of degradation can further be enhanced by addition of silver in the ZnO matrix (Figure 13 I).

Furthermore, so-generated catalyst was tested for decomposition of another industrially important dye used in textiles industry. Methyl orange (Figure 9c) is an anionic dye and can dissociate into organics under catalytic transformations. The amount of methyl orange absorbed by the catalyst is likely to be less due to presence of oxygen rich surfaces because of the negative charges on the catalyst surface [13]. Indeed, when ZnO alone was employed as a catalyst the degradation was poorer (only ~ 90% in 240 min) which however improved in presence of silver in ZnO confirming that presence of silver create scope for anionic dye to effectivel-

y absorb on the catalyst surface. Thus the complete reaction takes place (almost 100%) in 160 minutes as against 240 minutes of radiation with ZnO alone. The performance of plane ZnO in our case was still better than many reported articles thus further confirming that starch passivating ZnO surfaces are effective by themselves (Figure 13 II). Similarly, when the two catalysts studied in this work, were tested for degradation of Bromophenol Blue (Figure 9e), another anionic dye, the reaction rate was fast for Ag/ZnO than ZnO alone (Figure 14 I).

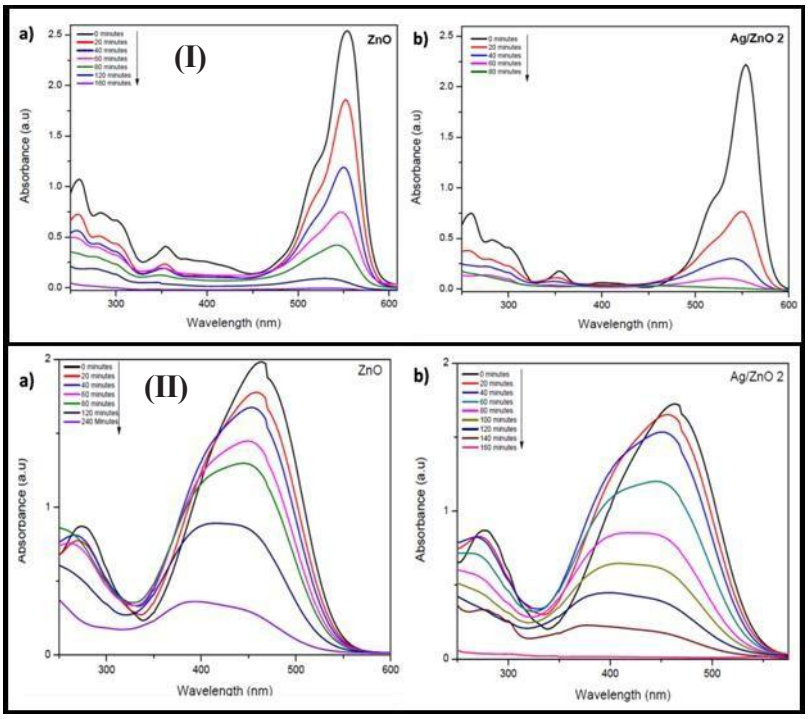

Figure 13: Photodegradation of (I) Rhodamine B, (II) MO using a) bare ZnO and b) Ag/ZnO 2

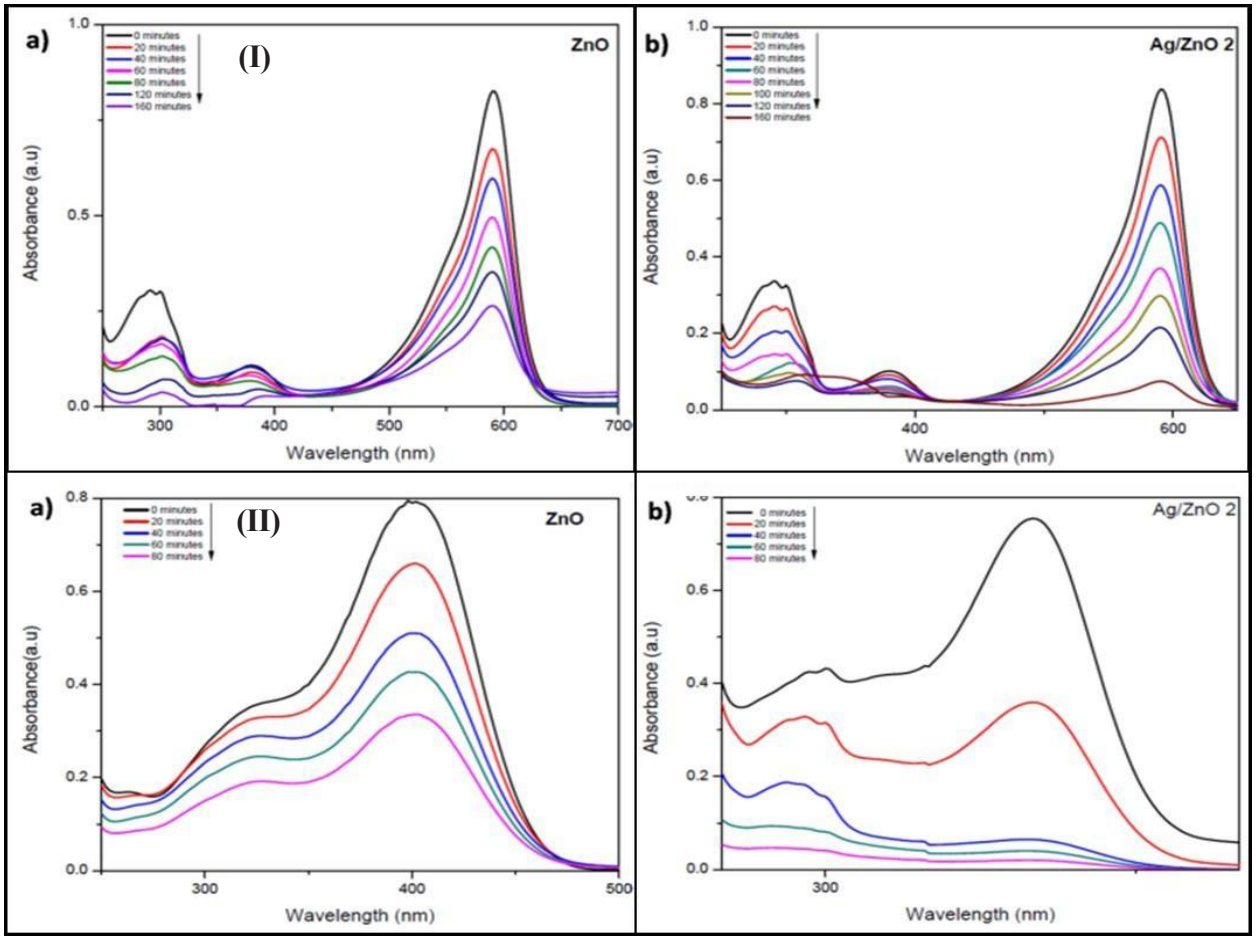

Figure 14: Degradation of (I) Bromophenol Blue, (II) p-nitrophenol using a) ZnO and b) Ag/ZnO **2**

Additionally, it is important in totality to understand need of effiuent treatment. There is large number of organic pollutants in industrial effiuent and providing a solution for total degradation of the contaminants, will obviously be a preferred technology. In order to establish the scope of current catalyst to have potential as a total solution, present article studies on phenol and phenolic compounds also which are common contaminants in industrial waste water. The degradation of phenols is challenging due to its stability and water solubility. For p-nitrophenol (Figure 9d) the reaction rates were very less for bare ZnO, the reaction was quite faster for Ag/ZnO. An intermediate peak, probably due to hydroquinone formation [45,46] is visible in the reaction for Ag/ZnO (Figure 14 II). By showing the efficiency of degradation for decomposition of five types of water pollutants, (Table 2) it is proposed that such type of catalyst can offer solution to water pollution problem that is a global concern.

Pollutants	Concentration of pollutants (mM)	Time for degradation (min)	Degradation (%) by	
			ZnO	Ag/ ZnO 2
Methylene Blue (MB)	0.02	120	90%	98%
Rhodamine B(RhB)	0.02	80	80%	99.9%
Methyl Orange(MO)	0.01	160	73%	98%
Bromophenol Blue (BPB)	0.005	160	64%	92%
p-nitrophenol (PNP)	0.01	80	70%	96%

Table 2: Efficiency of photocatalysts

Photocatalytic Mechanism

This research found that pure ZnO NPs exhibited strong photocatalytic activity. This is thought to be caused by two factors: first, the base material's high oxygen content narrowed the band gap, and second, dye sensitization excited the absorbed pollutant. Excess oxygen is evident in the catalyst sample, according to XPS and EDAX measurements. This is likely because starch has an oxidative function. A decrease in photocatalytic effectiveness may be seen when oxygen vacancies inside a ZnO crystal serve as recombination centers. Efficiency gains may be attributable to reduced recombination rates [2]. Possible low recombination rates and almost nonexistent impurity peaks are shown by the PL curve of ZnO. When exposed to visible light, chemisorbed dyes may be stimulated into single-and triple-states. To the conduction band of the semiconductor, electrons are transported from the excited dyes. Hydroxyl radicals are produced throughout the process and are responsible for advancing the degradation reaction [18].

When ZnO is doped with Ag, nano hetero junctions are formed. Optimum loading of Ag, as SEM and TEM data indicates, seems to be the reason for better photocatalytic property of 4% Ag/ZnO (Ag/ZnO 2) than 1% Ag/ZnO (Ag/ZnO 1). The electronic interaction in the metal semiconductor junction suppresses the recombination of the charge carriers. The current mechanism can be considered as similar to that has been reported by other researchers [42] where they have reported that due to localized surface plasmon resonance (LSPR) process, Ag particles act like an antenna for trapping sunlight radiation. LSPR acts as a locally excited electric field and the electrons in the valence band of excited silver nanoparticles (Ag* in reaction 6) get transferred to the conduction band of ZnO and showing formation of ZnO(e) [5]. Thereafter, ZnO in Ag/ZnO will transfer the charge to Ag NPs, thus increasing the rate of separation of photogenerated electron hole pairs. Holes in ZnO react with water leading to the formation of hydroxyl radicals and electrons in conduction band of Ag nanoparticle produce superoxide ($O_2^{\cdot-}$) radicals. These radical mineralize the pollutant molecules to basic substances [42,47]. The overall pictorial photocatalytic mechanism of degradation of MB in presence of Ag/ZnO under sunlight is shown in figure 15 [41]. The following reaction chain is the normal process [19,48];

$Ag + h\upsilon \rightarrow Ag^*$ .....(6)

$Ag^* + ZnO \rightarrow Ag^{\cdot+} + ZnO(e)$ .....(7)

$ZnO(e) + O_2 \rightarrow ZnO + O_2^{\bullet-}$ .....(8)

$O_2^{\bullet-} + H+ \rightarrow \bullet OOH$ .....(9)

$\bullet OOH + ZnO(e) + H^+ \rightarrow H_2O_2 + ZnO$ .....(10)

$H_2O_2 + ZnO(e) \rightarrow \bullet OH + OH^- + ZnO$ ..... (11)

Organic Pollutants + •OH (or •OOH) → Degraded Products .....(12)

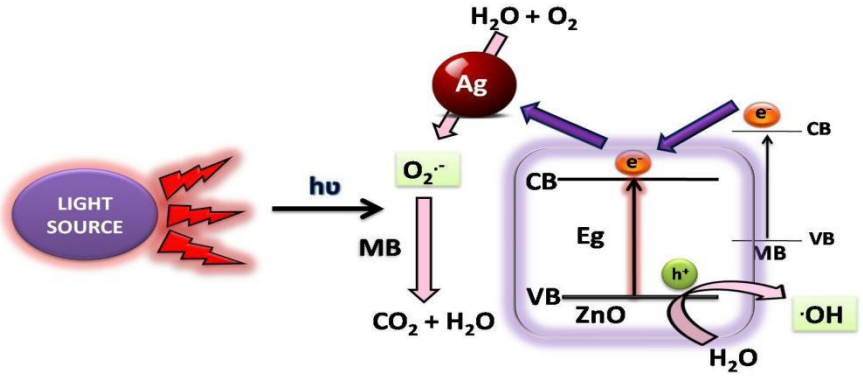

Figure 15: Proposed mechanism for degradation of MB *via* electronic events in presence of Ag/ZnO catalyst under sunlight

Additionally, in case of plasmonic photocatalyst (Ag/ZnO), intensive local electric field LSPR may create excitation of more electrons and holes and heat up the surrounding environment to increase the reaction rate and the mass transfer thereby polarizing the nonpolar molecules for better adsorption and absorption of pollutants with Ag/ZnO [30]. This local electric field may also have factored in better performance in the present study.

Conclusion

Starch was used to make an Ag/ZnO photocatalyst that is very efficient when exposed to sun light. During testing and assessment of its photocatalytic performance, the catalyst was characterized and found to have high crystalline characteristics as well as an excess of surface oxygen, both of which might be critical to the total catalytic activity. By increasing the band-gap towards the visible range, the presence of silver in the zinc oxide nanostructure transforms the UV-active zinc oxide into a visible light catalyst, allowing for its assessment under direct sunlight. There is evidence that silver improves photcatalysis and other surface qualities, such as dye absorption. In terms of catalyst ZnO, the photocatalytic activity was found to be best at 1 wt % Ag/ZnO 1 and 4 wt % Ag/ZnO 2, according to the comparative investigation. The rate was increased by 15% with 1% Ag/ZnO and by 40% with 4% Ag/ZnO. The Ag/ZnO 2 photocatalyst had the best performance (99.9% efficiency) when tested against rhodamine B. Methylene blue and rhodamine B were cationic dyes, whereas methyl orange, bromophenol blue, and p-nitrophenol were anionic dyes, all of which may be degraded by the catalysts that were thus produced. Even after the third cycle, it continued to exert its effects. An increase in the catalyst's potential industrial uses is the fact that it may be employed directly in sunlight.

References

1. The Electrochemical Photolysis of Water at a Semiconductor Electrode by Fujishima and Honda (1972). Page 37–38 of Nature 238. The authors of the 2011 paper "Oxygen Rich Titania: A Dopant Free, High Temperature Stable, and Visible Light Active Anatase Photocatalyst" are Etacheri, Seery, Hinder, and Pillai. Academic Journal of Functional Materials, 21(21), 3744–3752, 2017.b) "One-dimensional-based spatially ordered architectures for solar energy conversion" developed by Liu S, Tang ZR, Sun Y, Colmenares JC, and Xu YJ in 2015. The chemical society review, volume 44, pages 5053–5075. 3. A study conducted by Jag YJ, Simer C, and Ohm T (2006) compared the photocatalytic degradation of methylene blue using zinc oxide nanoparticles and its nano-crystalline particles. Mater Physical Review B, 41, 67–77. 4. a) Li et al. (2008) tested the photocatalytic degradation of phenol on TiO2 and ZnO in the presence of manganese dioxides; the results were compared. (Catal Today 139: 109–112). b) In 2015, Zhang et al. took a waltz using graphene as a platform to create composite photocatalysts. Yang, Liu, Sun, and Xu were the authors. Research in Chemistry 115: 10307–77. X. Zhou, G. Liu, J. Yu, and W. Fan (2012) Luminescent surface plasmon resonance photocatalysis using composites based on noble metals. Applied Mater. Sci. 22: 21337-84. The authors Primo, Corma, and García (2011) used titanium as a photocatalyst with gold nanoparticles. Phys Chem "Chemistry and Physics" 13: 886–9010. 7. Collado L., Jana P., Sierra B., Coronado J., Pizarro P., et al. (2013). Synergistic impact of Ag supported on TiO2 and ZnO semiconductors enhances hydrocarbon production by artificial photosynthesis. Citation: Chem Eng J 224: 128-35. Branched TiO2 nanorods for photoelectrochemical hydrogen generation. Nano lett 11: 4978-84. 8. Cho IS, Chen Z, Forman AJ, Kim DR, Rao PM, et al. (2011). 9. Ravishankar T, Manjunatha K, Ramakrishnappa T, Nagaraju G, Kumar D, et al. (2014). Zinc oxide nanoparticles doped with silver and those without were compared for their photocatalytic degradation of trypan blue. The article is published in Mater Sci Semicon Proc 36: 7-17. 9. In a 2014 study, Jasso-Salcedo, Palestino, and Escobar-Barrios developed Time, pH, and Ag on the formation of zinc oxide nanoagglomerates functionalized with Ag as photocatalysts. Published in the Journal of Catal Science 318: 170-8. 11. Wang Y, Wang Q, Zhan X, Wang, Safdar M, et al. (2013) Type II heterostructures powered by visible light and their improved photocatalytic capabilities: a comprehensive look. Nanoscale5, 8326–8339. 12. ekasuwandumrong O, Praserthdam P, Pratsinis SE, and Height MJ (2006) Developed Ag-ZnO catalysts for UV-photodegradation of methylene blue. Thirteen. Rauf M, Ashraf SS (2009) Basic concepts and practical uses of heterogeneous photocatalytic dye degradation in solution. Appl Catal B-Environ 63: 305-12. The photocatalytic breakdown process of methylene blue in water was described by Houas et al. (2001) in Chem Eng J 151: 10-8. Environmental and Applied Catalysis 31: 145–57. 15. Methods for activating TiO2 and ZnO with visible light, by Rehman, Ullah, Butt, and Gohar (2009).

Journal of Hazardous Materials 170: 560-9.